

Synthesis, Characterization, and Ion-Conductive Behavior in an Organic Solvent and in a Polyether of a Novel Lithium Salt of a Perfluorinated Polyimide Anion

Hiroyuki Tokuda,[†] Shunsuke Muto,[†] Nobuto Hoshi,[‡] Takashi Minakata,[‡] Masanori Ikeda,[‡] Fumihiko Yamamoto,[‡] and Masayoshi Watanabe^{*,†}

Department of Chemistry and Biotechnology, Yokohama National University, 79-5 Tokiwadai, Hodogaya-ku, Yokohama 240-8501, Japan, and Asahi Kasei Corp., 2-1 Samejima, Fuji-shi, Shizuoka 416-8501, Japan

Received November 1, 2001

ABSTRACT: To achieve highly conductive polymer electrolytes with a controllable ionic transference number, a novel polymeric lithium salt was synthesized and characterized. The novel lithium salt of a perfluorinated polyimide anion, poly(5-oxo-3-oxy-4-trifluoromethyl-1,2,4-pentafluoropentylene sulfonylimide lithium) (LiPPI), has a polyanionic backbone with a repeating unit resembling highly dissociable, thermally and electrochemically stable imide salts, such as lithium bis(trifluoromethylsulfonyl)imide (LiTFSI). The ion-conductive behavior of LiPPI in an organic solvent and in a polyether was extensively studied by using pulse-gradient spin-echo NMR, in addition to differential scanning calorimetry, complex impedance measurement, and dynamic mechanical analysis. Solutions of LiPPI in ethylene carbonate (EC) exhibited a high degree of dissociation and high ionic conductivity, and the self-diffusion coefficient of the anion was lower than that of the cation. Solvent-free polymer electrolytes were prepared by dissolving LiPPI in a matrix polyether to afford a compatible polymer alloy, and the ionic conductivity of the new polymer alloy electrolytes reached ca. 10^{-5} S cm⁻¹ at 30 °C. Although the lithium ionic transference number in the organic electrolyte solution was approximately the same as that of LiTFSI in EC, the polymer alloy electrolyte gave an apparent transference number higher than 0.7, which was considerably higher than that of LiTFSI in the same polyether.

1. Introduction

Solid polymer electrolytes are potentially applicable to many solid electrochemical devices such as high-energy-density batteries, electrochromic windows, and light-emitting devices.^{1–3} In most of the studies of polymer electrolytes, poly(ethylene oxide) (PEO) and its derivatives have been used as the matrix polyether, and monomeric lithium salts such as LiClO₄, LiBF₄, and LiN(SO₂CF₃)₂ (LiTFSI) are dissolved in the matrix polyether.^{1–3} In such polymer electrolytes, the polyethers preferentially interact with the cations and assist the dissociation of electrolyte salts and the lithium ion transport. On the other hand, the anions transport relatively freely in these systems. As a result, in polyether-based electrolytes, both cations and anions are mobile (bi-ionic conductors), and the lithium ionic transference number generally lies far below 0.5.

The strategies^{4–9} which have been reported to control the transference number can be roughly classified into two categories. In a “single ion conductor”, the anionic sites are anchored to the polymer backbone, so that only the cations are mobile.^{4–6} In the other, a “Lewis acidic anion receptor” is introduced into the electrolytes for the preferential interaction with the anion.^{7–9} In this way, both the ionic conductivity and the lithium ionic transference number are expected to be improved, by promoting the dissociation of electrolyte salts and by lowering the anionic mobility. These are certainly effective ways to control the transference number;

however, the conductivity, which is also an important property for solid polymer electrolytes, is much lower than that of bi-ionic conductors. A novel molecular design for polymer electrolytes with a controllable ionic transference number and high ionic conductivity is strongly desired for application of the polymer electrolytes to, for example, rocking-chair-type lithium batteries.

It has been reported that LiTFSI has striking characteristics, such as conformational flexibility and charge delocalization originated from the structure of the TFSI anion,^{10,11} to result in a high degree of dissociation even in low polar media like polyethers. We have proposed^{12,13} a novel strategy to control the ionic transference number of polymer electrolytes by using lithium salts of perfluorinated polyimide anions. The structure of the perfluoroimide anion like LiTFSI can play a role in promoting high dissociation. In addition, the polymeric structure allows the polyanion to have much higher molecular weight than Li⁺, so that the transference number can be controlled by the difference in mobility between Li⁺ and the polyanion.

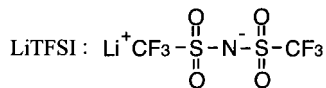
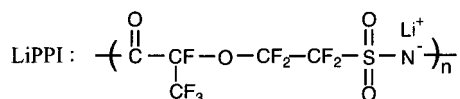
This concept led us to a novel lithium salt of a perfluorinated polyimide anion, poly(5-oxo-3-oxy-4-trifluoromethyl-1,2,4-pentafluoropentylene sulfonylimide lithium) (LiPPI). To enhance the electron-withdrawing effect of the sulfonylimide structure, a perfluorinated spacer chain is introduced (Figure 1). In addition, a spacer between the anionic sites decreases the charge density along the polymeric backbone to promote the ionic dissociation.¹³ It is expected that the polymer electrolytes having not only a high lithium ionic transference number but also high ionic conductivity are obtainable. In this paper, we describe the synthesis and

[†] Yokohama National University.

[‡] Asahi Kasei Corp.

* Corresponding author: Tel/Fax +81-45-339-3955; e-mail mwatanab@ynu.ac.jp.

Lithium Salts



Matrix Polymer

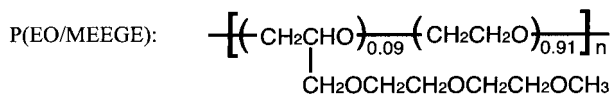


Figure 1. Structure of LiPPI, LiTFSI, and P(EO/MEEGE).

characterization of LiPPI. The properties of LiPPI as an electrolyte salt in an organic solvent and in a polyether are revealed by comparing with LiTFSI (Figure 1).

2. Experimental Section

2.1. Synthesis of a Novel Polymeric Lithium Salt.

LiPPI was prepared according to the procedure shown in Scheme 1. Tetrafluoroethylene and sulfuric acid anhydride were added to a pressure-proof container and mixed. After distilling the product, a small amount of triethylamine was added to the product under cooling, and fluorosulfonyldifluoroacetyl fluoride was obtained by a ring-opening reaction.¹⁴

Fluorosulfonyldifluoroacetyl fluoride (90 g), dried diethylene glycol dimethyl ether (60 mL), dried cesium fluoride (1.5 g), and hexafluoropropylene oxide (90 g) were added to a 300 mL shaker tube. This mixture was stirred for 4 h at 25–35 °C. The obtained product was ejected from the vessel and separated from the starting materials. After distillation, 2-(2-fluorosulfonyltetrafluoroethoxy)tetrafluoropropionyl fluoride (84.7 g, yield 56%, density 1.6 g cm⁻³ (25 °C), bp 87–89 °C) was obtained.

A solution, where 2-(2-fluorosulfonyltetrafluoroethoxy)tetrafluoropropionyl fluoride (69.2 g, 0.2 mol) was diluted with tetrahydrofuran (THF, 160 mL), was cooled to 0 °C, and a potassium bis(trimethylsilyl)amide (0.2 mol)/toluene solution (400 mL, 0.5 mol L⁻¹) was added dropwise to the solution over 1 h. This mixture was allowed to react for 7 h at 50 °C. Once the solvent was removed by vacuum distillation, *N,N*-dimethylacetamide (240 mL) was added and allowed to react for further 24 h at 165 °C. The deposited solid was filtered and dried at 120 °C under reduced pressure to yield a polymer (KPPI) as a light yellow solid.

An aqueous solution of the polymer was passed into a column packed with an ion-exchange resin (Organo, Amberlite IR-120B), and the column was washed by water. The collected aqueous solution was dried at 60 °C, and then, a light brown polymer (HPPI) was obtained (24 g). The obtained proton-type polymer (1.0 g) was dissolved in methanol (50 mL), and lithium carbonate was added with stirring over 90 min at ambient temperature to the solution. By complete evaporation of the solvent, a lithium salt (LiPPI) was obtained (1.1 g).

2.2. Preparation of Electrolyte Solutions and Solid Polymer Electrolytes. LiPPI and LiTFSI were used as electrolyte salts for electrolyte solutions and solid polymer electrolytes. LiTFSI (kindly supplied by IREQ) was dried under high vacuum at 120 °C for 12 h, and both of the lithium salts were stored in an argon atmosphere glovebox (VAC, [O₂] < 1 ppm, [H₂O] < 1 ppm). For electrolyte solutions, LiPPI and LiTFSI were dissolved in a polar aprotic solvent at different concentrations. Ethylene carbonate (EC), kept over molecular sieves (4 Å), was used for the solvent after distillation.

High molecular weight polyether comb polymer, poly[ethylene oxide-*co*-2-(2-methoxyethoxy)ethyl glycidyl ether],

P(EO/MEEGE) (Figure 1, kindly supplied by Daiso Co. Ltd.), which had been dried under high vacuum at 40 °C for 72 h and stored in the glovebox, was used as a matrix of solid polymer electrolytes. Given amounts of lithium salts and P(EO/MEEGE) copolymer were dissolved in anhydrous acetonitrile (Wako) to form a highly viscous homogeneous solution. The viscous solution was cast on a poly(tetrafluoroethylene) (PTFE) plate. To obtain homogeneous and flat films, the solvent was allowed to slowly evaporate at room temperature in the glovebox for several hours and then under high vacuum for 24 h.

2.3. Characterization of a Novel Polymeric Lithium Salt and Solid Polymer Electrolytes.

Gel permeation chromatography (GPC) was conducted on a Shimadzu LC-10 HPLC system with Shodex columns with 0.01 M LiCl *N,N*-dimethylformamide as the elution solvent. The columns were calibrated by poly(ethylene glycol) (PEG) standards (Tosoh). Potentiometric titration was carried out in order to obtain the structural information on HPPI. An aqueous solution of HPPI (0.0195 M based on the repeating unit, 75 mL) was titrated with NaOH (1 M); both the amount of added NaOH solution and the values of pH, monitored by a pH meter (HM-305 Toa Electronics Ltd.), were recorded. Differential scanning calorimetry (DSC) was carried out on a Seiko Instruments DSC 220C under a nitrogen atmosphere. Samples were sealed in Al pans in the dry glovebox, heated to 80 °C, quenched to -130 °C, and then heated at a rate of 10 K min⁻¹. The DSC thermograms were recorded during the programmed heating cycle. Thermogravimetry (TG) was measured on a Seiko Instruments TG-DTA 6200 under a nitrogen atmosphere at a heating rate of 10 K min⁻¹. Dynamic mechanical analysis (DMA) was performed on a Seiko Instruments DMS 210 under a nitrogen atmosphere at 10 Hz at a rate of 1 K min⁻¹.

2.4. Pulse Field Gradient Spin-Echo (PGSE) NMR

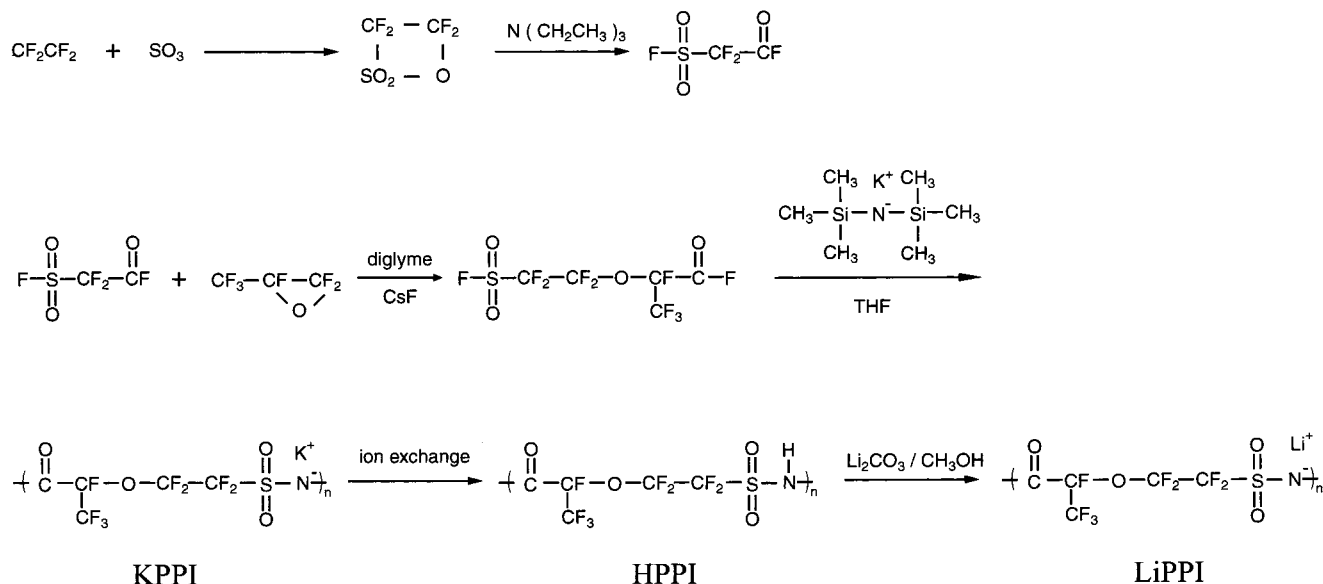
Measurement. The PGSE-NMR measurements were made by using a JEOL GSH-200 spectrometer with a 4.7 T wide bore superconducting magnet controlled by a TecMAG Galaxy system equipped with JEOL pulse field gradient probes and a current amplifier. Each electrolyte solution and polymer electrolyte were placed in a 5 mm (outer diameter) NMR microtube (BMS-005J, Shigemi, Tokyo) to a height of 5 mm. The length of the sample was intentionally made short so that it lay within the region of the constant magnetic field gradient. In electrolyte solutions, the self-diffusion coefficients were obtained at 40 °C and in polymer electrolytes at 60 °C. The ¹H and ⁷Li spectra were measured with a multiple-tuned PFG probe. The ¹⁹F spectrum was measured using a ¹⁹F/¹H probe. The gradient strength was calibrated and cross-checked using the known self-diffusion coefficient of H₂O at 30 °C (2.45 × 10⁻⁵ cm² s⁻¹).¹⁵ The measurements of the diffusion coefficients of the solvent, anion, and lithium ion were respectively made by ¹H, ¹⁹F, and ⁷Li NMR. The simple spin-echo pulse sequence was used for the diffusion measurements, and the free diffusion echo signal attenuation, *E*, is related to the experimental parameters by

$$\ln(E) = \ln(S/S_{g=0}) = -\gamma^2 g^2 D \delta^2 (\Delta - \delta/3) \quad (1)$$

where *S* is the spin-echo signal intensity, δ is the duration of the field gradient with magnitude *g*, γ is the gyromagnetic ratio, *D* is the self-diffusion coefficient, and Δ is the interval between the two gradient pulses.¹⁶ By plotting $\ln(S/S_{g=0})$ vs $\gamma^2 g^2 \delta^2 (\Delta - \delta/3)$, the self-diffusion coefficient can be derived from the slope of the resulting straight line.

2.5. Electrochemical Measurement. Ionic conductivity was determined by means of the complex impedance measurements with stainless steel blocking electrodes, using a computer-controlled Hewlett-Packard 4192A LF impedance analyzer over the frequency range from 5 Hz to 13 MHz. For electrolyte solutions, a sample was filled using a PTFE ring spacer (13 mm o.d., 7 mm i.d., 2 mm thickness). For polymer electrolytes, a film (0.2 mm thickness) was cut into disks of 10 mm diameter and put into a PTFE ring spacer (13 mm o.d., 10 mm i.d., 0.2 mm thickness). The electrolyte solution and polymer electro-

Scheme 1. Preparation of LiPPI



lyte films with the PTFE ring spacers, sandwiched between mirror-finished stainless steel electrodes, were sealed in PTFE containers in the glovebox and were subjected to the complex impedance measurements. The electrolyte solutions were measured at 40 °C, and the polymer electrolytes were measured from 100 to 0 °C under thermostated conditions.

The apparent transference number of the lithium ion in polymer electrolytes was determined by a combination of complex impedance and potentiostatic dc polarization measurements using the impedance analyzer, a dc voltage source (Advantest R6142), and a zero-shunt ammeter (Hokuto Denko HM-103). The polymer electrolytes sandwiched between metallic lithium electrodes were sealed in polypropylene (PP) containers. The dc polarization at 10 mV was conducted at 60 °C to record change in the polarization current, after measuring the complex impedance.

3. Results and Discussion

3.1. Characterization of a Novel Polymeric Imide Salt. The reduced viscosity of KPPI, 0.30 dL g⁻¹ (30 °C, in THF), indicates that the precursor monomer was polymerized, and the polymer included potassium at 10.2 wt % (calculated for KPPI: 10.8 wt %) by elemental analysis. For the IR spectrum of the polymer, absorbance at 1689 and 1620 cm⁻¹, at 1327 and 1299 cm⁻¹, and at 1160 cm⁻¹, attributable to the C=O stretching vibration mode, the SO₂ stretching, and the C-F stretching, respectively, were observed. The ¹⁹F NMR spectrum (methanol-*d*₄, δ from C₆F₆) showed peaks at δ = 82, 80, 48, and 33 ppm, which can be assigned to CF₃, CF₂O, SO₂CF₂, and CF, respectively. From these results, it can be confirmed that the synthesized polymer has the structure (–COCF(CF₃)–OCF₂CF₂SO₂NK–) as the repeating unit. The IR spectrum for the polymer passed through the ion-exchange resin showed N–H stretching and deformation vibration mode at 3365 and 3290 cm⁻¹, and the ¹H NMR spectrum (methanol-*d*₄, δ from TMS) exhibited a signal at δ = 8.2 ppm, assignable to N–H. These measurements indicate that KPPI, which has the unit of (–COCF(CF₃)OCF₂CF₂SO₂NK–), changed to (–COCF(CF₃)OCF₂CF₂SO₂NH–), namely, HPPI.

To obtain information on the structure of HPPI, the potentiometric titration measurement was performed (Figure 2). It was expected that the equivalent point, which could be estimated by the concentration (0.0195

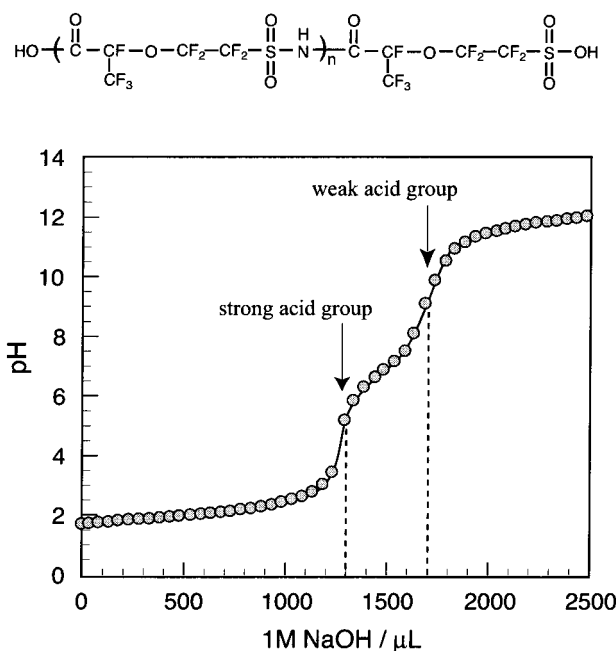


Figure 2. Potentiometric titration curve of aqueous solution of HPPI using 1 M NaOH and proposed structure of HPPI.

M) and the amount (75 mL) of an aqueous solution of HPPI used for the titration and formula weight per unit (323.07), would be 1460 μL. The pH titration curve shows double equivalent points, and the titration volume up to the second equivalent point (1700 μL) is larger than the calculated titration volume (1460 μL), as seen in Figure 2. The first equivalent point (1300 μL) corresponds to 76.5% of the total titration volume (1700 μL). We assume here that the profile of the titration curve arises from the relatively small molecular weight of HPPI which has terminals of sulfonic acid and carboxylic acid, respectively (Figure 2), and that these end acidic groups contribute to the titration. It seems that the first equivalent point in Figure 2 corresponds to the neutralization of amide acid (–SO₂NHCO–) and end sulfonic acid (–SO₃H), which are strong acid groups in the polymer structure, and the difference between the first and second equivalent points corresponds to

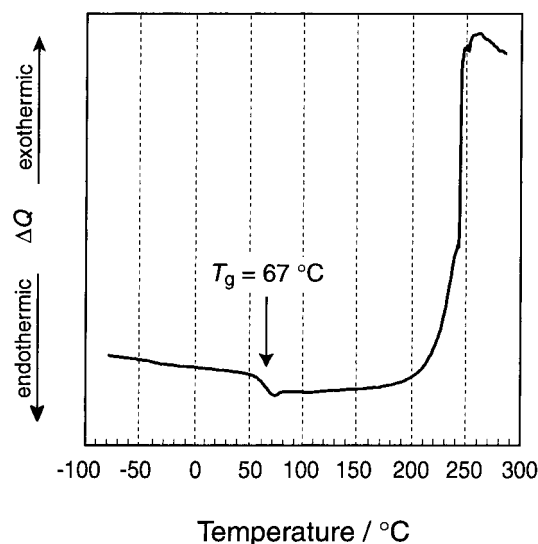


Figure 3. DSC thermogram of LiPPI at a heating rate of 10 K min⁻¹.

the neutralization of the remaining end carboxylic acid (–COOH), considered to be a weak acidic group. On the basis of this assumption, we estimated the molecular weight of HPPI by the following equation:

$$0.765(n + 2) = n + 1$$

where n is the number of the amide acid group, i.e., the degree of polymerization. The result of this calculation shows that the degree of polymerization of the novel polyanion is 2.26 and that the number-average molecular weight (M_n) is 1072. pH of the HPPI aqueous solution (0.0195 M based on the repeating unit) was found to be 1.71. Since the pH value calculated from this M_n , assuming complete dissociation of the amide acid and sulfonic acid groups, is 1.76, our assumption regarding the molecular structure of HPPI is considered to be valid. It is confirmed that the newly synthesized HPPI is a polyelectrolyte having strong acid groups. The molecular weight of the polyelectrolyte was also characterized by GPC using LiPPI. The weight-average molecular weight and number-average molecular weight were found to be 9.6×10^3 and 8.4×10^3 . The molecular weight determined by GPC was much larger than that by the titration. We believe that the GPC molecular weight is less reliable, because polyelectrolytes frequently have large excluded volumes due to electrostatic repulsion between the charged sites, whereas GPC standards, in this case PEG's, are nonionic.

To evaluate thermal stability of the novel lithium salt of the polyimide anion, LiPPI, DSC, and TG measurements were performed. A heat capacity change assignable to a glass transition temperature (T_g) of LiPPI appears at 67 °C, and LiPPI is stable until ca. 200 °C (Figure 3). In addition, the weight change in a high-temperature range was examined by TG (not shown). A 10% weight loss was not observed until about 250 °C. These results show that LiPPI has thermal stability up to 200 °C.

The electrochemical stability of LiPPI in EC was investigated by cyclic voltammetry at a Ni electrode with a Li reference and counter electrode. From this cyclic voltammogram (data not shown), plating and stripping of lithium were clearly seen in the cathodic limit. In the reverse anodic scan, irreversible oxidation

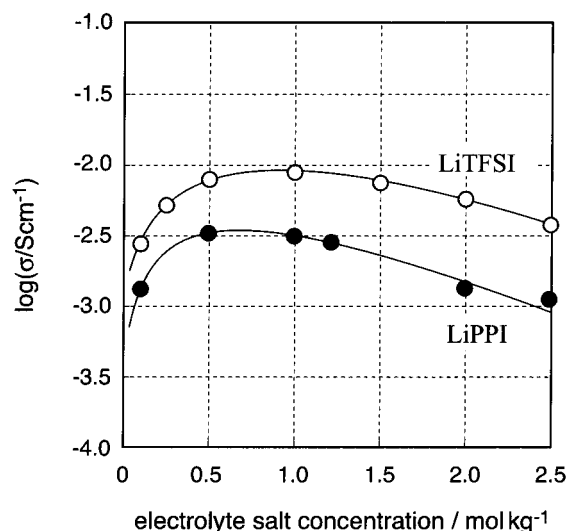


Figure 4. Ionic conductivities at 40 °C for ethylene carbonate solutions containing either LiPPI or LiTFSI as a function of electrolyte salt concentration.

was observed at ca. 5 V. Consequently, it is confirmed that the novel lithium salt of the polyimide anion, LiPPI, is stable up to ca. 5 V vs Li/Li⁺.

3.2. Ion Conductive Behavior in Organic Solutions. Figure 4 shows ionic conductivities at 40 °C of EC solutions containing either LiPPI or LiTFSI as a function of the electrolyte salt concentration. In general, ionic conductivity of an electrolyte solution passes through a maximum with increasing electrolyte salt concentration. For low salt concentrations, increase in the conductivity is due to an increase in the number of charge carriers. With increasing concentration, ionic association and viscosity increase of the solutions take place mainly due to enhancement of ion–ion interaction. At the maximum point of ionic conductivity (0.5 mol kg⁻¹), the novel polymeric lithium salt, LiPPI, exhibits a conductivity of 3.0×10^{-3} S cm⁻¹. On the other hand, LiTFSI shows an ionic conductivity of 7.5×10^{-3} S cm⁻¹ at the same salt concentration.

To microscopically understand such difference in the ionic conductivity of the LiPPI and LiTFSI solutions, we performed PGSE-NMR measurements. Figure 5 shows the attenuation of the intensity of the ¹H, ⁷Li, and ¹⁹F PGSE-NMR echo spectra of the LiTFSI-EC solution (a) and the LiPPI-EC solution (b) vs $\gamma^2 g^2 \delta^2 (\Delta - \delta/3)$. The slopes of these plots give the diffusion coefficients (see eq 1). For the LiTFSI-EC solution, the self-diffusion coefficient follows the order EC > anion > lithium. The lithium ion, having a high surface charge density, strongly interacts with ethylene carbonate by ion–dipole interaction. Consequently, the hydrodynamic radius becomes larger than that of the highly charge-delocalized TFSI anion, which weakens the interaction with the solvent. However, the diffusion coefficient of the LiPPI-EC solution is described in the following order: EC > lithium > anion. This result means that the anionic diffusion is suppressed by the polymerized structure, which seems to have a much larger hydrodynamic radius than the lithium ion solvated by EC.

Table 1 shows the self-diffusion coefficients of the solvent (EC), lithium, and anion obtained by PGSE-NMR, and the ratio of lithium diffusion coefficient ($D_+/ (D_+ + D_-)$), for the electrolyte solution containing either LiTFSI or LiPPI. On comparing the LiPPI-EC and LiTFSI-EC solutions, the LiTFSI solution exhibits

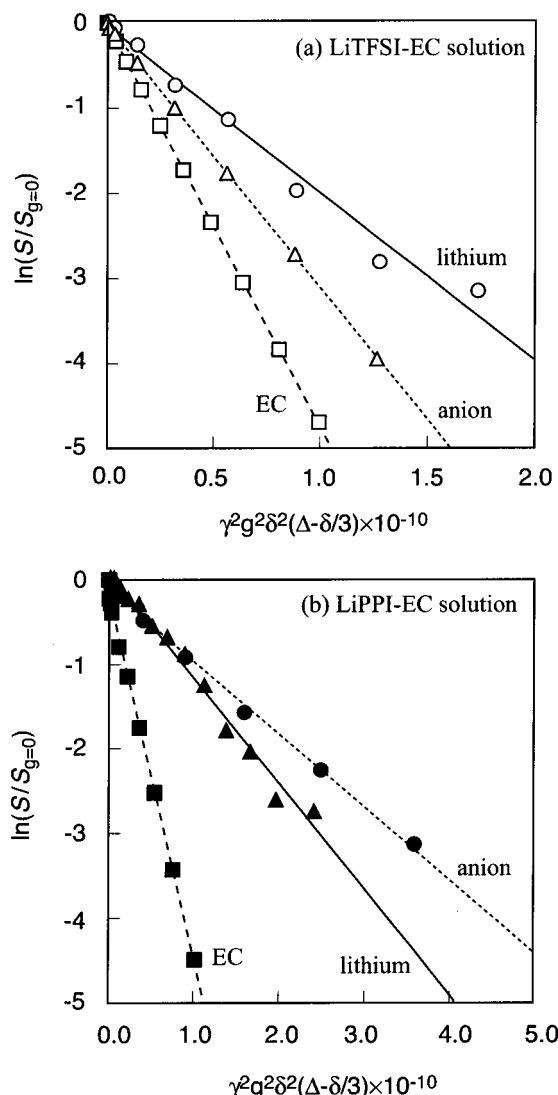


Figure 5. Signal attenuation plots of ^1H (EC), ^7Li (lithium), and ^{19}F (anion) NMR echo spectra in ethylene carbonate (EC) vs $\gamma^2 g^2 \delta^2 (\Delta - \delta/3)$ at 40 °C: (a) LiTFSI-EC solution; (b) LiPPI-EC solution.

Table 1. Self-Diffusion Coefficients, the Ratio of Lithium Diffusion Coefficient to the Summation of Lithium and Anionic Diffusion Coefficients, ($D_+/D_+ + D_-$), Apparent Degree of Dissociation, α , and Presumed Lithium Ionic Transference Number, t_+ , for EC-Based Electrolyte Solutions Containing Either LiPPI or LiTFSI (0.5 mol/kg) at 40 °C

| | diffusion coeff/ $10^{-6} \text{ cm}^2 \text{ s}^{-1}$ | | | $D_+/(D_+ + D_-)$ | α | t_+ |
|--------|--|-------|---------|-------------------|----------|-------|
| | EC | anion | lithium | | | |
| LiPPI | 4.28 | 0.86 | 1.25 | 0.59 | 0.58 | 0.37 |
| LiTFSI | 4.72 | 3.09 | 1.96 | 0.39 | 0.60 | 0.39 |

higher self-diffusion coefficients for all the measured nuclei than the LiPPI solution. Although these systems are too concentrated to be regarded as a dilute solution, the ionic diffusion coefficient, D , is assumed to relate to the Stokes–Einstein equation:

$$D = \frac{kT}{6\pi\eta r_s} \quad (2)$$

where η is the solution viscosity, r_s is the effective hydrodynamic (Stokes) radius, and k is the Boltzmann constant. The difference in diffusion coefficients between

the LiPPI and LiTFSI solutions is caused by the variation in both viscosity and the Stokes radius. However, the difference in the anionic diffusion coefficients is apparently much larger than that in the diffusion coefficients of other measured nuclei, which indicates that the anionic diffusion coefficient is decreased by the polymerized anionic structure. This is supported by comparison of $D_+/(D_+ + D_-)$, which clearly suggests that anionic diffusion of LiPPI is inhibited by the polymerized anionic structure. In addition, the $D_+/(D_+ + D_-)$ for LiPPI electrolyte solution higher than 0.5 shows that ionic diffusion for the LiPPI system is dominated by the lithium ion.

From the self-diffusion coefficients by the PGSE-NMR measurements, the ionic conductivity can be calculated according to the Nernst–Einstein equation:

$$\sigma_{\text{diff}} = \frac{Nq^2}{kT}(D_+ + D_-) \quad (3)$$

where N is the number of charge carriers per cm^3 on the assumption of complete dissociation, q is the electronic charge on each charge carrier, and D_+ (D_-) is the diffusion coefficient of the cation (anion), respectively. Since the PGSE-NMR measurement observes NMR-sensitive nuclei, the diffusion coefficients are average values between dissociated and associated ionic species in the system. Therefore, it is possible to roughly estimate the degree of ionic dissociation (α) from the ratio of the calculated conductivity value (σ_{diff}) and the value measured by complex impedance (σ_{imp}) by the following equation:

$$\alpha = \frac{\sigma_{\text{imp}}}{\sigma_{\text{diff}}} \quad (4)$$

Since the ionic transference number is defined by the ratio of ionic mobility, the lithium ionic transference number, t_+ , can be estimated by the following equation:

$$t_+ = \frac{\mu_+}{\mu_+ + \mu_-} = \frac{q_+ D_+}{q_+ D_+ + q_- D_-} \quad (5)$$

where μ_+ (μ_-) and q_+ (q_-) are ionic mobility and electronic charge on the cation (anion), respectively. For the PPI anion, because of having multicharge on its backbone, the anionic charge, q_- , is concerned with the degree of dissociation in the solvent. Thus, q_- is estimated by multiplying the degree of dissociation and the number of anionic sites along the polymeric structure determined by the potentiometric titration measurement. The calculated results are also shown in Table 1. It is interesting to note that the apparent degree of dissociation of LiPPI is comparable to that of LiTFSI, which indicates that LiPPI is highly dissociable, probably due to the anionic charge delocalization similarly to LiTFSI. Also, it can be seen that the apparent lithium ionic transference number of LiPPI is approximately the same value as that of LiTFSI. These results indicate that decrease in the ionic conductivity for the LiPPI-EC solutions (see Figure 3) can be mainly attributed to diminution of the ionic mobility. The reason for no increase in t_+ for LiPPI is explained as follows. The ionic mobility, μ , is given by the Stokes equation:

$$\mu = \frac{q}{6\pi\eta r_s} \quad (6)$$

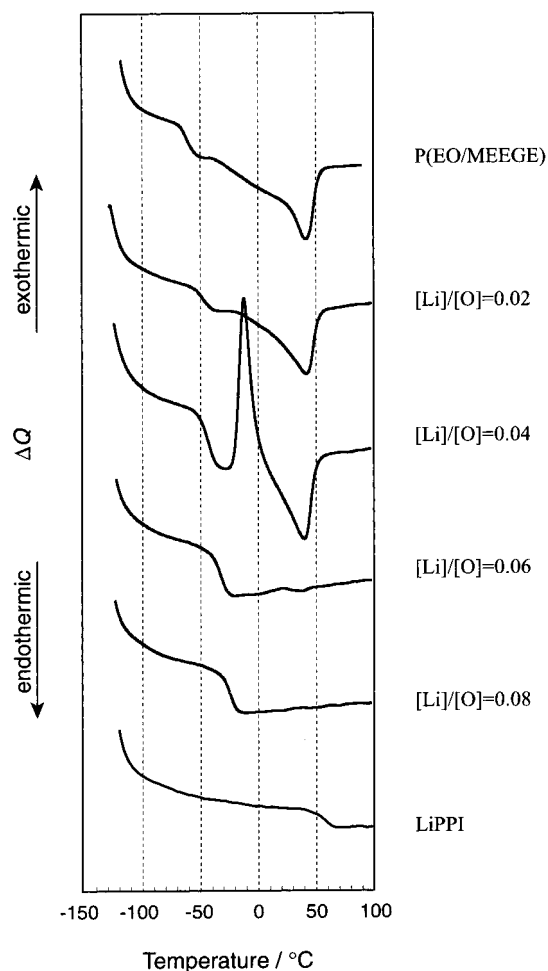


Figure 6. DSC thermograms of P(EO/MEEGE) containing LiPPI at a heating rate of 10 K min⁻¹.

Equation 6 suggests that the polymerization of the anionic unit is related with the increases not only in its Stokes radius but also in its charge on the anionic backbone. The balance of the two factors affects the ionic transference number.

3.3. Characterization of Polymer Electrolytes.

The polymer electrolytes prepared by dissolving LiPPI in P(EO/MEEGE) gave translucent or transparent films. DSC thermograms of P(EO/MEEGE), LiPPI, and its polymer electrolytes containing LiPPI are shown in Figure 6. In these polymer electrolytes, heat capacity changes, attributable to T_g of LiPPI, do not appear at 67 °C. With increase in the concentration of the dissolved polymeric lithium salt, the crystallinity is further reduced and T_g is raised. In general, it is difficult for two different polymers to be compatible with each other. It is important to know whether LiPPI is completely compatible with the matrix polyether, P(EO/MEEGE). To explore compatibility between P(EO/MEEGE) and LiPPI in detail, dynamic mechanical analysis (DMA) was carried out. Figure 7 shows the tensile modulus (E') and loss tangent ($\tan \delta$) of P(EO/MEEGE) and its polymer electrolytes containing LiPPI ([Li]/[O] = 0.04 and 0.08) at 10 Hz as a function of temperature. For the matrix polyether, the main relaxation in E' and the main peak seen in $\tan \delta$ at ca. -60 °C can be assigned to its T_g . When LiPPI is dissolved in the polyether matrix, the E' relaxation and $\tan \delta$ peak temperatures are also increased, and the $\tan \delta$ peaks are clearly seen as a single peak. The E' value of P(EO/MEEGE) at

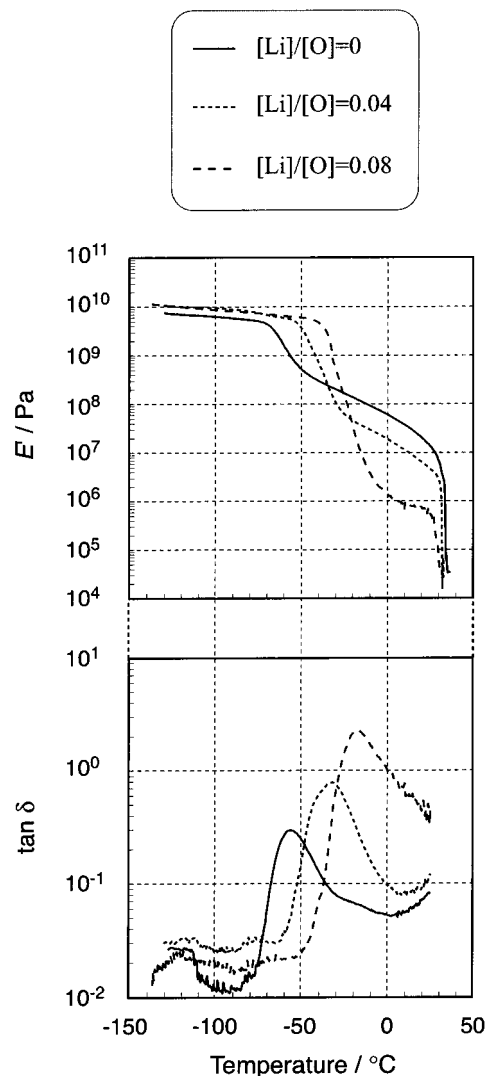


Figure 7. Tensile modulus (E') and loss tangent ($\tan \delta$) for P(EO/MEEGE) containing LiPPI at 10 Hz as a function of temperature.

ambient temperature is still on the order of 10⁷ Pa due to the crystallinity, where the crystallites function as physical cross-linking points of the polymers. With the increase in LiPPI concentration of its polymer electrolytes, decrease in the E' value at ambient temperature can be seen. This behavior, i.e., the increase in T_g and reduced crystallinity of P(EO/MEEGE), indicates that conformation change of the matrix polyether is inhibited because of the coordination of the ether structure to the doped lithium salt.^{1,2} From both the DMA and DSC spectra, it is seen that the completely amorphous polymer electrolytes were obtained at a concentration of [Li]/[O] = 0.06–0.08. It can be concluded that the polymeric lithium salt, LiPPI, is compatible with the matrix polyether. Polyethers are quite strong donors (Lewis base) similar to glymes; however, they have low permittivity and very poor accepting property, so they lack hydrogen bonding for anionic solvation.¹ The main reason for the compatibility between LiPPI and P(EO/MEEGE) seems to be resulted from ion–dipole interaction between the polyether and the lithium ion with which the polyanion interacts by Coulombic interaction.

Figure 8 shows T_g of the polymer electrolytes containing either LiPPI or LiTFSI, determined by DSC, plotted against lithium salt concentration. The T_g curves appear

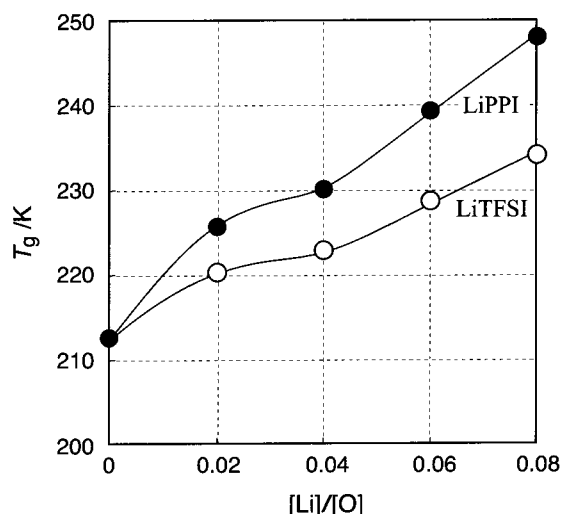


Figure 8. Glass transition temperature for P(EO/MEEGE) containing LiPPI and LiTFSI as a function of electrolyte salt concentration.

to be similar in the way they rise. However, the magnitude is different, despite having similar anionic structures. It is known that LiTFSI moderately raises the T_g of its doped polymer electrolytes, compared with other monomeric lithium salts.^{10,11} This behavior has been explained by charge delocalization of the TFSI anion, which promotes dissociation and weakens the basicity and the interaction with the matrix polyether chains. The charge delocalization has been ascribed to strong electron-withdrawing effect of the $-\text{SO}_2\text{CF}_3$ group. These characteristics may be reflected in the weak interaction of the TFSI anion with the polyether matrix. The PPI anion also has a structure promoting the electron-withdrawing effect; however, it apparently differs from the TFSI anion in terms of having the polyanionic charge separated by a perfluorinated spacer chain, the $-\text{CF}(\text{CF}_3)\text{OCF}_2\text{CF}_2-$ group. The local anionic charge density along the PPI structure in the polyether is much higher than that of the TFSI anion in the same matrix, even if the apparent concentration of the lithium salts ($[\text{Li}]/[\text{O}]$) is the same. This fact may enhance ion-ion interaction in the polymer electrolytes containing LiPPI. The compatibility between the PPI anion and the matrix polyether seems to mainly evolve from the indirect interaction mediated by the lithium ion. Thus, the segmental motion and relaxation of the matrix polyether are affected not only by the polyanion-polyether interaction but also by the ion-ion interaction, which leads to the larger increase of T_g in the polymer electrolytes containing LiPPI. The nonlinear increase in T_g for both of the polymer electrolytes as a function of the salt concentration, seen in Figure 8, can be understood by considering the partially crystalline nature of the low-concentration electrolytes, in which the lithium salts are excluded from the crystallites to the amorphous region of the polymers.

3.4. Ionic Conductivity and Lithium Ionic Transference Number for Polymer Electrolytes. The P(EO/MEEGE) copolymer, used as the matrix polyether for polymer electrolytes in this study, has a fairly high molecular weight ($M_w = 1.5 \times 10^6$, $M_w/M_n = 5.4$) and a low degree of crystallinity ($\approx 14\%$, determined by DSC) caused by introducing 2-(2-methoxyethoxyethyl) glycidyl ether (MEEGE) units.¹⁷ In addition, since the short and flexible ether side chain contributes to fast molecular motion, we have reported^{17,18} that the polymer electro-

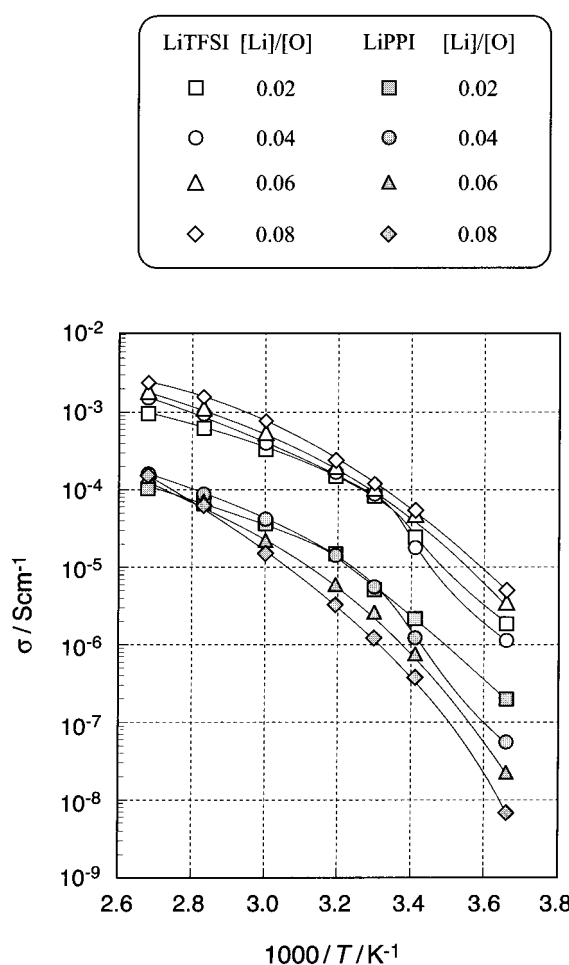


Figure 9. Arrhenius plots of ionic conductivity for P(EO/MEEGE) containing LiPPI and LiTFSI.

lytes based on P(EO/MEEGE) copolymers exhibit much higher ionic conductivity compared with PEO and its derivatives. Figure 9 shows temperature dependences of ionic conductivities for the polymer electrolytes containing either LiPPI or LiTFSI. All of the Arrhenius plots of the ionic conductivity exhibit positively curved profiles, as can be expressed by the Williams-Landel-Ferry or Vogel-Tamman-Fulcher equation. In some polymer electrolytes, the temperature dependences are deviated from the smoothly changed curved profile, and steep drops of the ionic conductivity are observed below ambient temperature. These deviations can be attributed to crystallization of the polymer electrolytes and well coincides with the DSC results (Figure 6: the DSC spectra of LiTFSI electrolytes are not shown). The ionic conductivity at 30 °C for LiPPI electrolytes shows a maximum at $[\text{Li}]/[\text{O}]$ concentration ratio of 0.04; on the other hand, for LiTFSI electrolytes at $[\text{Li}]/[\text{O}] = 0.08$ (see Figure 9).

When $[\text{Li}]/[\text{O}] = 0.04$, it is evident that the polymer electrolyte containing LiPPI exhibits lower ionic conductivity than that containing LiTFSI by approximately 1 order of magnitude. For polymer electrolytes containing lithium salts, the proportion of the conductivity transported by the lithium ion, i.e., lithium ionic transference number (t_+), is a significant parameter, which determines performance of the polymer electrolytes when they are applied to electrochemical devices. In this study, apparent t_+ was estimated for the polymer electrolytes containing LiPPI and LiTFSI by a combina-

Table 2. Apparent Lithium Ionic Transference Number for P(EO/MEEGE) Electrolytes Containing Either LiPPI or LiTFSI ([Li]/[O] = 0.04) at 60 °C

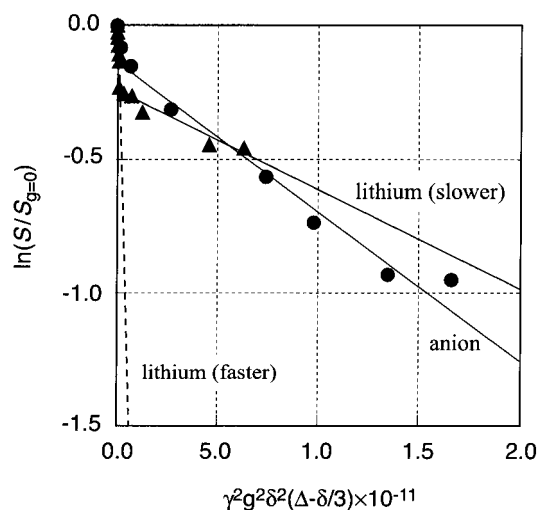
| Li salts | LiPPI | LiTFSI |
|-------------------|-------|--------|
| t_{Li^+} | 0.75 | 0.07 |

tion of ac impedance measurement and potentiostatic polarization measurement.^{19,20} The transference number is given by the following equation:

$$t_+ = R_b / [V/I(\infty) - R_i] \quad (7)$$

where R_b and R_i are respectively bulk resistance and interfacial resistance obtained from the complex impedance measurements, and V and $I(\infty)$ are respectively applied potential and steady-state limiting current, for the potentiostatic polarization measurements. Table 2 shows an apparent lithium ionic transference number for the polymer electrolytes containing either LiPPI or LiTFSI. It can be seen that the LiTFSI system gives a very low value, which indicates that the ionic conductivity is dominated by anionic mobility. The characteristics of the TFSI anion (vide supra) allow facile ion dissociation of LiTFSI and weak interaction of the TFSI anion with polyether solvent dipoles, which is in fact confirmed by the low T_g (Figure 8), high ionic conductivity (Figure 9), and very low apparent transference number (Table 2). On the other hand, the polymer electrolyte containing LiPPI exhibited a higher t_{Li^+} value than 0.7. This high value reveals that ionic conductivity of the LiPPI system is dominated by lithium cationic motion, in contrast with the LiTFSI system. The difference in ionic conductivities between the LiPPI and LiTFSI systems can mainly be attributed to the relative difference in anionic mobility.

3.5. Ion-Conductive Behavior of LiPPI in an Organic Solvent and in a Polyether. The lithium salt of a novel polyanion, LiPPI, exhibited ionic conductivity of ca. 10^{-5} S cm⁻¹ as well as a much higher apparent lithium ionic transference number than LiTFSI, by alloying it with a matrix polyether, P(EO/MEEGE). The difference in the transference number values between LiPPI and LiTFSI in the polyether is in contrast with the approximately same transference number values in an organic solution, EC. Figure 10 shows the attenuation of the intensity of the ⁷Li and ¹⁹F PGSE-NMR echo spectra of P(EO/MEEGE) containing LiPPI ([Li]/[O] = 0.04) vs $\gamma^2 g^2 \delta^2 (\Delta - \delta/3)$ at 60 °C. It can be seen that the attenuation of the intensity of the anion is not a completely straight line as the electrolyte solution plots (Figure 5), but it slightly bends down. Hayamizu et al. recently reported that the ¹⁹F NMR echo decay signal of the anions was obtained as single attenuation in the plots for solvent-free polymer electrolytes containing LiTFSI.²¹ It seems reasonable to consider the curved ¹⁹F plots are caused by molecular weight distribution of the polymeric PPI anion. Therefore, the ¹⁹F echo signals were approximated as a single-exponential decay, and an average diffusion coefficient was obtained from the slope ($D_- \approx 6 \times 10^{-8}$ cm² s⁻¹). On the other hand, it can be seen that the attenuation of the intensity of ⁷Li is clearly approximated by two straight lines. This result indicates that the diffusion of lithium is composed of two diffusion species. One lithium component shown by the dashed line is a faster diffusive species ($D_+ \approx 9 \times 10^{-7}$ cm² s⁻¹), and the solid line component is a slower one ($D_+ \approx 5 \times 10^{-8}$ cm² s⁻¹). Moreover, the slopes between the slower lithium com-

**Figure 10.** Signal attenuation plots of ⁷Li (lithium) and ¹⁹F (anion) NMR echo spectra of P(EO/MEEGE) containing LiPPI ([Li]/[O] = 0.04) vs $\gamma^2 g^2 \delta^2 (\Delta - \delta/3)$ at 60 °C.

ponent and the anionic species are not so much different, compared with the difference between the two lithium components. These results seem to indicate that the diffusion component of the slower species corresponds to the lithium ions associated with the polyanion in these polymer electrolytes. In addition, the faster lithium diffusion species originated from the dissociated lithium ion in this system seems to dominate the ionic conductivity. This hypothesis is in accord with the results of the apparent lithium ionic transference number determined by the electrochemical measurement (Table 2).

It is important to remember that the lithium ionic transference number of LiPPI in EC was approximately the same as that of LiTFSI, as shown in Table 1. The large difference in the transference number of LiPPI, depending on the solvents, seems to be ascribed to the differences in (a) dielectric constant of each solvent and (b) viscosity (i.e., free volume) in each system. EC, a low molecular weight organic solvent, has a very high dielectric constant ($\epsilon = 89.6$; 40 °C); however, polyether has a quite low value ($\epsilon \approx 5$). The difference in dielectric constant affects the dissociation of an electrolyte salt in each system. In the solution system, LiPPI largely dissociates, and the PPI anion more strongly receives the migration force from the electric field, allowing enhancement of its mobility. In terms of the free volume, a solid polymer electrolyte has much less free volume than an electrolyte solution. The free volume theory²² predicts that diffusivity of small particles, like ions, in glass-forming liquids greatly diminishes with decrease in the free volume. The diffusivity is also dependent on the size of the diffusing species and exponentially decreases with increasing size. The effect of the molecular size of the PPI anion on the diffusivity seems to be more pronounced in the polyether solvent than in EC.

4. Conclusion

A novel lithium salt of a perfluorinated polyimide anion, LiPPI, having high thermal and electrochemical stability, was synthesized. The concept to obtain polymer electrolytes with a controllable ionic transference number by keeping moderate ionic conductivity was demonstrated by alloying LiPPI in a polyether matrix. LiPPI was compatible with the polyether, and the

resulting polymer electrolytes were allowed to have ionic conductivity of ca. 10^{-5} S cm $^{-1}$ at 30 °C, being dominated by lithium ion conduction. This clearly contrasted with a monomeric lithium salt, LiTFSI, in the same polyether. The high lithium ionic transference number for LiPPI may be attributed to the large size of the PPI anion embedded in a low free volume medium and by low permittivity of the polyether matrix. Polymer electrolytes obtained by dissolving a monomeric lithium salt in a polyether have been extensively studied, and increase in the ionic conductivity has been achieved to some extent. However, the studies have revealed an inconsistent result, namely, that when there is an enhancement of the ionic conductivity, there is a decrease in the lithium ionic transference number. We expect that the incorporation of polymeric lithium salts can be a new concept for novel molecular design to achieve compatibility between high ionic conductivity and high lithium ionic transference number.

Acknowledgment. This research was supported in part by Grant-in-Aid for Scientific Research on Priority Areas (A) "Molecular Synchronization for Design of New Material System" (No. 404/11167234) from the Japanese Ministry of Education, Science, Sports and Culture and NEDO International Joint Research Grant. The authors thank Dr. Kikuko Hayamizu, National Institute of Materials and Chemical Research, for the help and discussion in PGSE-NMR measurements, and we are grateful to Daiso. Co. Ltd. for supplying us valuable chemicals for our research.

References and Notes

- (1) *Polymer Electrolyte Reviews 1 and 2*; MacCallum, J. R., Vincent, C. A., Eds.; Elsevier: London, 1987, 1989.
- (2) Gray, F. M. *Solid Polymer Electrolytes*; VCH Publishers: New York, 1991.
- (3) *Application of Electroactive Polymers*; Scrosati, B., Ed.; Chapman & Hall: London, 1993.
- (4) Benrabah, D.; Sylla, S.; Alloin, F.; Sanchez, J.-Y.; Armand, M. *Electrochim. Acta* **1995**, *40*, 2259.
- (5) Onishi, K.; Matsumoto, M.; Nakacho, Y.; Shigehara, K. *Chem. Mater.* **1996**, *8*, 469.
- (6) Fujinami, T.; Tokimoto, A.; Mehta, M. A. *Chem. Mater.* **1997**, *9*, 2236.
- (7) Lee, H. S.; Yang, X. Q.; Xiang, C. L.; McBreen, J. *J. Electrochem. Soc.* **1998**, *145*, 2813.
- (8) Mehta, M. A.; Fujinami, T. *Chem. Lett.* **1997**, 1997, 915.
- (9) Zhang, S. S.; Angel, C. A. *J. Electrochem. Soc.* **1996**, *143*, 4047.
- (10) Vallée, A.; Besner, S.; Prud'homme, J. *Electrochim. Acta* **1992**, *37*, 1579.
- (11) Armand, M.; Gorecki, W.; Andrèani, R. *Second International Symposium on Polymer Electrolytes*; Scrosati, B., Ed.; Elsevier: New York, 1990; p 91.
- (12) Watanabe, M.; Suzuki, Y.; Nishimoto, A. *Electrochim. Acta* **2000**, *45*, 1187.
- (13) Watanabe, M.; Tokuda, H.; Muto, S. *Electrochim. Acta* **2001**, *46*, 1487.
- (14) England, D. C.; Dietrich, M. A.; Lindsey, R. V., Jr. *J. Am. Chem. Soc.* **1960**, *82*, 6181.
- (15) Weingärtner, H. *Z. Phys. Chem.* **1982**, *132*, 129.
- (16) Stejskal, E. O. *J. Chem. Phys.* **1965**, *43*, 3597.
- (17) Nishimoto, A.; Watanabe, M.; Ikeda, Y.; Koujiya, S. *Electrochim. Acta* **1998**, *43*, 1177.
- (18) Nishimoto, A.; Agehara, K.; Furuya, N.; Watanabe, T.; Watanabe, M. *Macromolecules* **1999**, *32*, 1541.
- (19) Watanabe, M.; Nagano, S.; Sanui, K.; Ogata, N. *Solid State Ionics* **1988**, *28–30*, 911.
- (20) Kato, Y.; Watanabe, M.; Sanui, K.; Ogata, N. *Solid State Ionics* **1990**, *40/41*, 632.
- (21) Hayamizu, K.; Aihara, Y.; Price, W. S. *J. Chem. Phys.* **2000**, *113*, 4785.
- (22) Cohen, M. H.; Turnbull, D. *J. Chem. Phys.* **1959**, *31*, 1164.

MA011904N